Featured in Physics

Material-Independent Mechanochemical Effect in the Deformation of Highly-Strain-Hardening Metals

Anirudh Udupa,[1,*] Koushik Viswanathan,[1] Mojib Saei,[1] James B. Mann,[2] and Srinivasan Chandrasekar[1]

[1] *Center for Materials Processing and Tribology, Purdue University, West Lafayette, Indiana, 47907, USA*
[2] *Department of Mechanical Engineering, University of West Florida, Pensacola, Florida, 32514, USA*

(Received 19 November 2017; revised manuscript received 22 March 2018; published 13 July 2018)

Soft and highly-strain-hardening metals such as iron, aluminum, and tantalum, often called "gummy," are notoriously difficult to cut. This is due to their tendency to exhibit redundant, unsteady plastic flow with large-amplitude folding, which results also in macroscale defects on the cut surface and large energy dissipation. In this work, we demonstrate that this difficulty can be overcome by merely coating the initial metal surface with common adhesive chemical media such as glues and inks. Using high-speed *in situ* imaging, we show that the media act by coupling unsteady surface-plastic-flow modes with interface energetics—a mechanochemical action—thereby effecting a ductile-to-brittle transition, locally. Consequently, the unsteady plastic flow with folding transitions to a periodic segmentation-type flow in the presence of the surface media, with near absence of defects on the cut surface and significantly lower energy dissipation (a reduction of up to 80%). This mechanochemical effect is controllable and not material specific, with the chemical media demonstrating comparable efficacy across different metal systems. This makes it quite distinct from other well-known mechanochemical effects, such as liquid-metal embrittlement and stress-corrosion cracking, that are both highly material specific and catastrophic. An analytic model incorporating local flow dynamics, stability of dislocation emission, and surface-media energetics is found to correctly predict the onset of the plastic-flow transition. The benign nature and simplicity of the media suggest wide-ranging opportunities for improving the performance of cutting and deformation processes for metals and alloys in practical settings.

DOI: 10.1103/PhysRevApplied.10.014009

I. INTRODUCTION

It is well known that soft metals, as well as metals with a large strain-hardening capacity, such as pure aluminum, iron, copper, and tantalum, are notoriously difficult to cut. This difficulty is manifest as very large forces, thick chips, and a profusion of defects on the surface [1,2]; hence, such soft metals are often called "gummy" [3]. It was shown recently that this difficulty is due to an unsteady mode of large-strain plastic deformation—sinuous flow, characterized by plastic buckling and large-amplitude material folding—that prevails during cutting [2,4–6]. If this sinuous flow mode can be disrupted and replaced by a more favorable deformation mode, with smaller forces and deformation strain, then cutting of these metals could be carried out efficiently.

A possible general route for modulating plastic flow in cutting or processing is via utilization of mechanochemical effects—changes in the mechanical response of a material in the presence of a chemical medium. Mechanochemical effects have been known in some form or the other for a long time, the earliest reports perhaps dating back nearly 2000 years to the use of Hg by Roman gold miners [7]. The mechanochemical route has been exploited in processing of ceramics and other nonmetals; examples include chemomechanical planarization [8,9] and comminution [10,11]. In metals, mechanochemical effects are regarded as being highly material specific and almost synonymous with catastrophic failure, e.g., stress-corrosion cracking and liquid-metal embrittlement [12–16]. A few chemical media such as CCl_4 [17–20] have shown promise in favorably influencing metal-cutting processes, speculated to occur via changes in the metal's ductility [21–23]. However, there are concerns about variability in reports of these effects [24–26]. Additionally, these media have critical health and environmental issues (e.g., CCl_4 is a well-known carcinogen) that far overshadow any potential utility.

Given the uncertainty in using controllable mechanochemical effects in metals, we recently revisited the role of

*audupa@purdue.edu

surface-active (SA) chemical media in influencing large-strain plastic flow in metals. *Surface active* is a term conventionally used to describe those media that form a strong adsorbed layer on metal surfaces and influence surface energies [24,27]. We found that when a common metal-marking ink was coated, prior to cutting, onto the surface of commercially pure copper (which deforms by sinuous flow in the annealed condition), the cutting forces are lowered significantly [2]. This preliminary observation pointed to the more wide-ranging possibility of certain adsorptive media influencing the plastic-flow process in the cutting of metals, in hitherto, unknown ways. The present work is thus an outgrowth of these preliminary observations.

In this study, we demonstrate profoundly beneficial mechanochemical effects in large-strain deformation of metals using very common media such as commercial glue sticks and marking inks. The effects are shown to arise from a strong coupling between these media and the underlying plastic-flow mode. The effects are widespread, controllable, materially agnostic, and with scope for practical application. The demonstration is an outcome of a multiscale reexamination of mechanochemical phenomena in deformation of metals, using high-resolution *in situ* and *ex situ* observations.

The paper is organized as follows. The experimental setup is described in Sec. II. The primary observations of the mechanochemical effect are presented in Secs. III A–III D and an analytic model explaining the physics behind the effect is described in Sec. III E. The implications of our study are discussed in Sec. IV and concluding remarks are presented in Sec. V.

II. EXPERIMENTAL PROCEDURES

Preliminary cutting experiments with commercially pure copper have shown that application of some common chemical media to the metal surface prior to the cutting caused reductions in the cutting force and energy [2]. These effects appear to depend also on the initial strain-hardening state of the copper, with the media effect being significant in annealed copper. Motivated by these observations, the experimental program is structured (1) to study the effects of various chemical media, characterized by different adhesive coupling strengths to metal surfaces, on plastic flow and cutting; and (2) to examine how these effects are influenced, if at all, by the initial hardening state (e.g., annealed or prehardened) of the metal. This program structure thus enables exploration of hypotheses pertaining to how media effects occur and whether these are coupled to specific flow phenomena.

The model 2D cutting system consists of a ductile, highly-strain-hardening metal workpiece cut by a hard wedge (tool) at constant velocity V_0. The tool is fixed normal to V_0, and has a constant penetration depth h_0 (see Fig. 1). As a result, a part of the workpiece material is removed in the form of a chip (strip) of thickness h_C by plastic deformation (strains >2). This system is well established also as a means for imposing varying extents (controlled) of large-strain shear deformation [2]. The flow of metal in the deformation or cutting zone is observed *in situ* and captured using a high-speed camera, with images postprocessed using digital-image-correlation (DIC) techniques to obtain quantitative flow-field information (e.g., displacement or strain history, material rotation, or flow lines) [28].

Three different workpiece materials, well known for their strain-hardening capacity, are used in the cutting experiments: commercially pure Cu (99.99% oxygen-free high-conductivity Cu 101), commercially pure Al (99% Al 1100), and commercially pure Fe (99.85% American Rolling Mill Company (ARMCO)). The copper and iron samples are machined to dimensions of $75 \times 25 \times 6$ mm^3 before annealing in an inert atmosphere (argon). The copper is annealed at 750 °C for 4 h and oven cooled, while the iron is annealed at 950 °C for 4 h and oven cooled. Annealing in the inert atmosphere minimizes the formation of an oxide layer on the metal surface. The hardness of annealed Cu is 68 Vickers hardness (HV) and that of annealed Fe is 90 HV. The aluminum samples are directly procured as sheets in the annealed (O) and the half-hard (H14) state. The latter enables study of flow-media coupling effects arising from prehardening of the metal before cutting. The dimensions of the aluminum workpieces are $100 \times 25 \times 1.5$ mm^3. The hardness of the annealed Al is 23 HV and that of the half-hard (H14) Al is 30 HV.

A range of chemical media are used to coat the workpiece surface prior to cutting, with the coated surface remote from the tool-chip contact (Fig. 1, left). The selection of these media, to test various hypotheses underlying mechanochemical effects and flow, is based on considerations such as the strength of their adhesive bonding via physical adsorption to the metal surface, and the chemical specificity of the bonding to the metal surface. Based on this interaction strength, the media are broadly classified into three groups:

(1) *Group I* consists of media that show strong physical adsorption to the three metals. The following media belong to this group: glue 1 (Scotch restickable glue stick), glue 2 (Scotch Super Glue Gel), glue 3 (Gorilla Super Glue), ink 1 (Sharpie permanent marker), ink 2 (Dykem, and ink 3 (Paper Mate Liquid Paper correction fluid).
(2) *Group II* consists of media that show chemical affinity (specificity) for Al only, as established by their ability to corrode oxide-free Al surfaces. The following media belong to this group: isopropyl alcohol (Fisher Chemical), ethanol (Decon Labs), and 1-butanol (Fisher Chemical).
(3) *Group III* consists of media that are not known for any significant adsorptive or other similar interactions with any of the metals. The following media belong to this

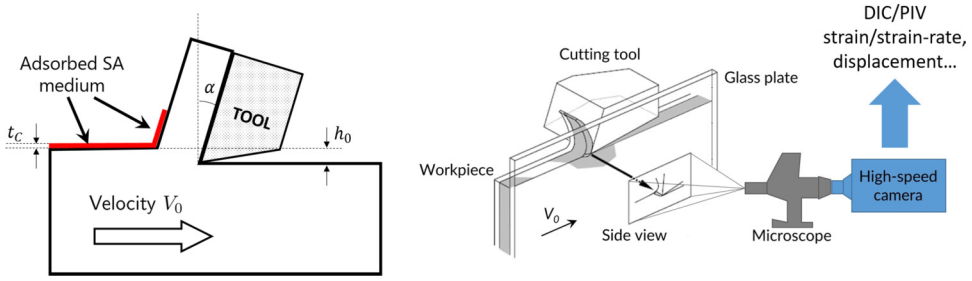

FIG. 1. Schematic of cutting configuration used in the experiments. The SA medium is applied to the workpiece free surface remote from the tool-chip interface. The deformation zone is observed *in situ* to obtain high-resolution quantitative flow-field information.

group: distilled water, toluene (Consolidated Chemical), and acetone (Fisher Chemical).

Additionally, some other media, which could not be clearly classified into one of the aforementioned groups, are also studied. These include soap (Proctor & Gamble), paraffin wax (Gulf Wax), adhesive tape (Scotch transparent tape), and diacetone alcohol (Lab Alley).

The cutting is carried out using a tungsten carbide tool, carefully ground so that the cutting edge has a radius of less than 5 μm. The width of the rake face of the tool is 2.3 mm, which also corresponds to the chip width into the plane in Fig. 1. The initial cutting depth h_0 is fixed at 50 μm, while the cutting speed V_0 is fixed at either 2 or 15 mm/s, with no effect on the results. The low V_0 minimizes any temperature effects on the deformation. In order to ensure plane-strain deformation, side flow of the workpiece material is prevented using a quarter-inch glass plate as a lateral constraint. The media are applied to the top surface of the workpiece as shown in Fig. 1. The region of interest, illuminated by halogen white light (150 W), is imaged using a high-resolution CMOS camera (pco.dimax), coupled to an optical microscope (Nikon Optiphot), with a resolution of 1.4 μm per pixel and a frame rate of 200 frames/s. A piezoelectric dynamometer (Kistler 9254) is used to measure the cutting forces, with the data sampled at 900 Hz. The specific energy for cutting could be obtained from the measured force and cutting speed. The topographical characteristics of the residual cut surface are evaluated using a large-area three-dimensional (3D) optical profilometer (Zygo NewView 8300).

The cutting is carried out both with and without a lubricant applied to the cutting zone. The lubricant, when used, is Mobil 1 High Mileage 5W-30. The primary observations are unchanged in the presence of the lubricant, precluding any potentially obscuring effects due to lubrication.

III. RESULTS

The high-speed imaging has enabled quantification of the flow during deformation, both with and without SA media application. We present the primary experimental results below, followed by an analytic model that captures the essential physics underlying the mechanochemical effect with SA media.

A. Sinuous flow, SA media, and plastic-flow transition

Sinuous plastic flow, an unsteady flow mode characterized by repeated material folding and large local strains, is the norm when cutting soft and highly-strain-hardening metals [2,6]. The highly redundant deformation, due to folding, results in large cutting forces, energy dissipation, and a very thick chip [4,6]. This type of flow is nucleated by a plastic-buckling instability on the material free surface [5]: see the top row of Fig. 2, which shows three frames from a high-speed *in situ* image sequence. A bump, with extremities P_1 and P_2 termed pinning points, results from plastic buckling on the free surface; P_1 and P_2 are almost always coincident with grain boundaries and/or other local heterogeneities [5,29]. As deformation continues, the bump grows in size, and is rotated, eventually evolving into a large-amplitude fold. The process repeats with subsequent buckling events leading to adjacent folds collapsing onto each other to form the chip, as reflected by the wavy streaklines in the images.

In the presence of SA media, applied remote from the tool-workpiece interface, a distinct deviation from sinuous flow is observed—a mechanochemical effect. Three frames from a high-speed sequence showing the resulting deformation for annealed Cu with an SA medium (glue 1) are presented in the bottom row of Fig. 2. The plastic-buckling instability, with bump formation, again occurs ahead of the tool: see the pinning points Q_1 and Q_2 in frame 1. However, during the initial stages of the bump developing into a fold, a crack now nucleates on the free surface at the pinning point Q_1 and propagates toward the tool tip (red arrow, frame 2). This crack propagates to varying degrees, depending on the cutting conditions (α, V_0, h_0), before it is arrested (frame 3). Subsequently, another plastic-buckling event is initiated and the process repeats. The development of sinuous flow with folding is thus disrupted by a "segmented" type of flow, caused by recurring fracture in the presence of the SA medium. This transition in flow, observed with several other SA media, characterizes the mechanochemical effect. Video 1 explicitly demonstrates the transition in annealed Cu with an SA medium (glue 1) coated along the latter half of its length.

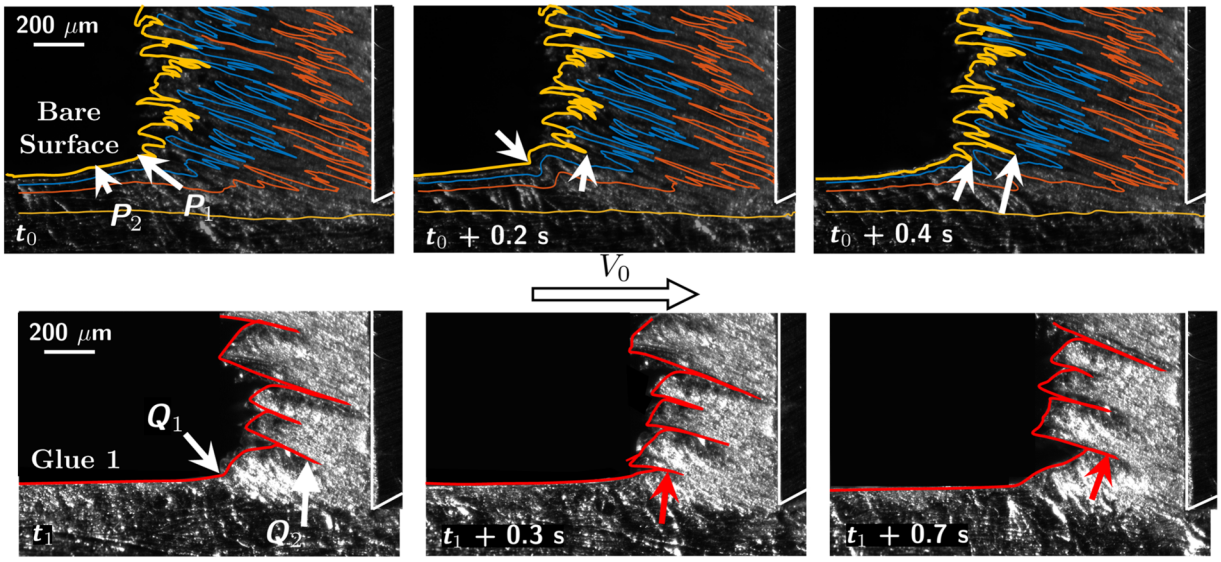

FIG. 2. High-speed *in situ* images of the deformation zone in cutting of annealed Cu. (Top row) Three frames from a sequence showing sinuous flow, absent any SA medium. This flow is characterized by large-amplitude material folding, as revealed by the wavy streaklines in the workpiece. Each folding event is initiated by a buckling instability leading to formation of a surface bump bound by pinning points P_1 and P_2 (arrows, frame 1). The bump grows in size and evolves into a fold (frames 2 and 3) and the process repeats. (Bottom row) When an SA medium (glue 1) is applied to the Cu surface remote from the tool-chip contact, buckling still occurs: see the bump bounded by pinning points Q_1 and Q_2 (frame 1). However, a fracture instability now sets in before the bump evolves into a fold, and a crack grows from the pinning point Q_1 (red arrow, frame 2). The crack is arrested close to the tool tip (frame 3); the chip is much thinner, consisting of a series of segments with each segment resulting from a crack. This type of flow is called segmented-type flow.

The transition in plastic flow, from sinuous to segmentation-type when the SA media is applied, is manifested in the resulting chip. Not only is the chip now much thinner than before (cf. Fig. 2, top and bottom rows), but the morphology on its free surface is also much altered (see Fig. 3). The characteristic mushroom-type structure [Fig. 3(a)] with sinuous flow, absent any media, is due to adjacent folds that have collapsed onto each other (yellow arrows). With the SA medium present, the chip instead has a sequence of periodically spaced "segments" [Fig. 3(b)], with fractured surfaces (red arrows) dominating over regions with minor folding events (yellow arrows). Crucially, crack-initiation sites coincide with the pinning points that bound the initial bump (Q_1, Q_2 in Fig. 2). Locally, these regions are shaped like notches and result in a sharp stress concentration. It is interesting that in cases where sinuous flow is absent, thereby precluding any such stress concentrators, the SA media have no influence

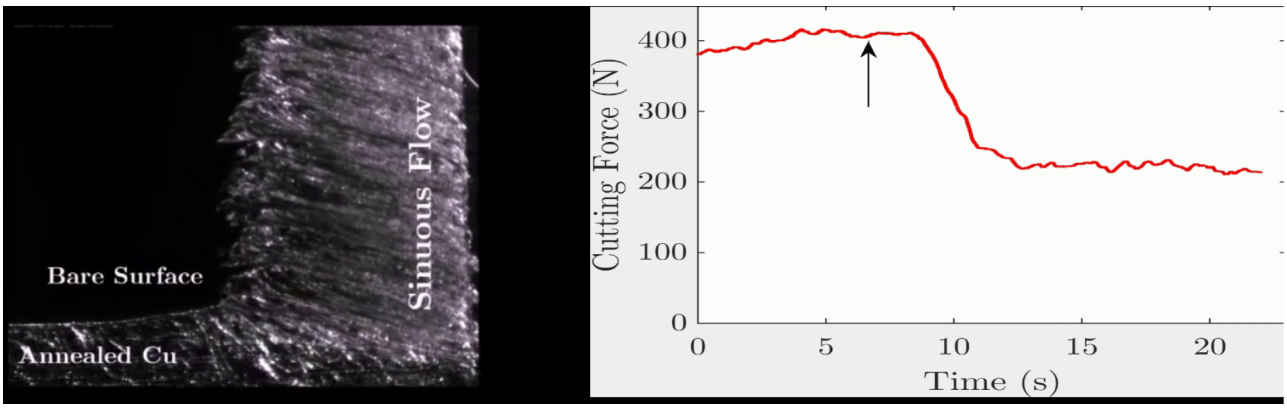

VIDEO 1. Transition from sinuous to segmentation-type flow due to SA media application. Annealed Cu is cut initially with an uncoated surface, resulting in sinuous flow, a thick chip, and a large cutting force. The latter half of the workpiece free surface (remote from the tool-chip interface) is coated with glue 1, resulting in a transition to segmentation-type flow, a thin chip, and a much reduced cutting force. Simultaneous variation in the force is shown on the right.

on the process at all. This is illustrated by applying the same medium to the metal in an initially fully hardened state (prestrain ∼2.5). Here, it is known that the tendency for plastic buckling is much reduced [2,5] and that the resulting flow is laminar or smooth—a fact that remains unchanged by the medium application.

B. Effect of group-I–III media on forces and energy dissipation

Perhaps the most drastic consequence of the mechanochemical effect is a consistent reduction in cutting force accompanying the change in flow or chip morphology. We test the three metal systems with 16 different common media, and varying tool rake angle $\alpha = 0^\circ, 45^\circ$ and initial workpiece conditions—annealed and half-hard (H14) (see Sec. II for details). In each case, the SA medium is applied on the metal's free surface, remote from the tool-chip contact interface (see Fig. 1). Figure 4 is a scatter plot of the absolute magnitude of the corresponding cutting forces (parallel to the velocity V_0 direction) when cutting bare uncoated metal (F_B) and the coated samples (F_C). Data are shown for Al and Cu, and with $\alpha = 0^\circ$. The different metal-media combinations appear to be enveloped between the lines $F_C = F_B$ (no mechanochemical effects) and $F_C = 0.2F_B$ (largest reduction, ∼80%).

Based on the data in this figure, the SA media may be classified into three groups. Group-I media show consistent mechanochemical effects and force reductions independent of the metal to which they are applied (see Fig. 4). Examples in this group include commercial glues, glue 1 (Scotch glue) and glue 2 (Gorilla Super Glue), and metal-marking inks, ink 1 (Sharpie) and ink 2 (Dykem). The corresponding force reduction is ∼50% ($F_C = 0.5F_B$), corresponding to the points clustered around the $F_C = 0.5F_B$ line in the figure. The force reduction in each case is accompanied by a corresponding transition from sinuous to segmented-type flow (see Video 1). All of the media in this category are distinguished by their ability to adhere well to metal surfaces [30].

Group-II media show pronounced effects only with some metals, and group-III media show no effects at all ($F_C = F_B$ in Fig. 4). For instance, alcohols in group II—isopropyl alcohol (IPA), butyl alcohol, and ethanol—show the largest force reductions (nearly 80%, $F_C = 0.2F_B$) with Al, yet had no effect with Cu. This is noteworthy since isopropyl alcohol, in particular, is the only common ingredient of media in group I (e.g., inks 1 and 2), yet shows no effect with Cu and Fe (unlike inks 1 and 2 themselves). Again, this is reflective of the strength or weakness of local adhesive bonds that form at the media-metal interface: the alcohols are known to form strong bonds with Al to such an extent that they may even corrode it to form the corresponding alkoxide [31,32]. Likewise, distilled water and toluene (group III, little to no adhesion) show no effects at all with any of the metals. Note that the points clustered around $F_C = F_B$ consist of group II (with Cu) and group III (both Al and Cu) media.

A more expansive set of results with all three metals (Cu, Al, and Fe) and $\alpha = 0^\circ$,45° is shown in Fig. 5. In addition to confirming the general trends discussed in Fig. 4, the bar chart also shows larger force reductions when $\alpha = 0^\circ$ ($F_C \sim 0.5F_B$) compared to $\alpha = 45^\circ$ ($F_C \sim 0.8F_B$). This may be directly attributed to the increased propensity for sinuous flow at $\alpha = 0^\circ$, i.e., a larger fold amplitude and a thicker chip. This is also confirmed by comparing the forces for the annealed vs the half-hard initial state (see Al H14 in Fig. 5), since the latter is well known to exhibit laminar, instead of sinuous, flow [2,5]. Since both the total energy dissipated and the specific energy (energy per unit volume) of deformation are directly proportional to the cutting force, the force reductions indicate a reduction in the specific energy. Furthermore, the energy reduction reflects the reduced strains accompanying segmented flow in the presence of SA media.

C. Flow perturbation due to localized media application

To further demonstrate the mechanochemical effect of SA media, two other sets of experiments are carried out, as shown in Fig. 6. In the first, the initial half-length of the workpiece (Cu) is kept uncoated, thereby presenting fresh annealed material to the cutting tool; and the SA medium (ink 1) applied only to the latter half of the workpiece length ([see inset to Fig. 6(a)]. All other experimental conditions are unchanged. As expected, when cutting the uncoated or bare region, the forces are quite high ($F_B =$ 500 N) and a sharp reduction occurrs when the tool traverses the coated region of the workpiece. In the second demonstration, periodically spaced spots of an SA medium (ink 1) are placed on the workpiece (annealed Al) surface along the sample length [see inset to Fig. 6(b)]. The resulting force then oscillates between a high F_B and a low F_C, the oscillation frequency matching the spatial frequency of the spot pattern. These observations are quite repeatable with all the media that demonstrate significant mechanochemical effects.

D. Surface defects and topography

Alongside the transition in flow mode and the attendant force reduction, the SA medium application is found to result in a remarkable improvement in quality of the newly created (cut) workpiece surface. As has been demonstrated clearly elsewhere, the occurrence of folding and sinuous flow is synonymous with the formation of pits, cracks, and tears on the resulting surface [28,33]. Figure 7(a) shows a 3D surface profile of a typical pit on the newly generated Cu surface arising from the folding process. The ratio of pit size (maximum depth from free surface) to initial tool penetration depth is $\Delta_P/h_0 \sim 0.75$, and the average pit area

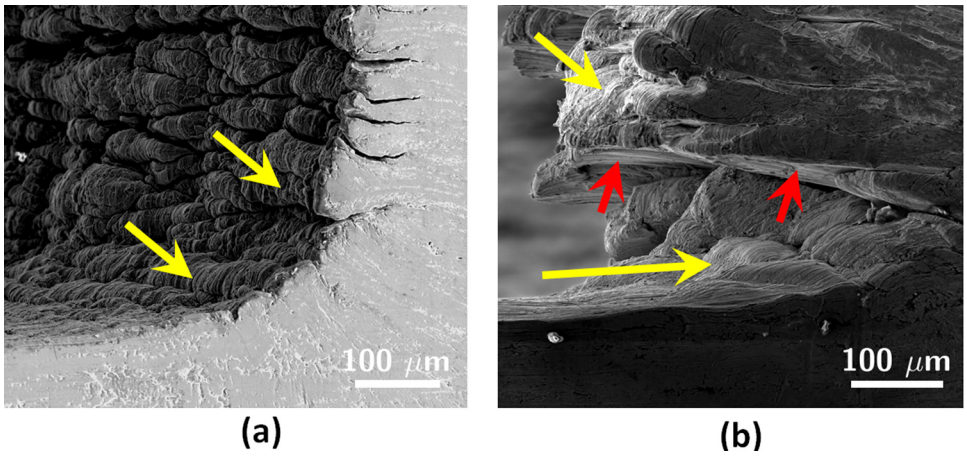

FIG. 3. Scanning electron microscopy images of chip morphology in Cu. (a) Characteristic mushroom-type structures on the chip free surface, a signature of sinuous flow, arise due to individual folds (yellow arrows) collapsing onto each other. (b) In the presence of an SA medium (glue 1), the flow transitions from sinuous to segmentation type, characterized by minor folding events in each segment (yellow arrows) and separated by periodic fracture surfaces (red arrows). The morphologies span the entire width of the chips.

and density are $3.3 \times 10^4\ \mu\text{m}^2$ and $6.2/\text{mm}^2$, respectively, reflecting significant degradation of the newly formed surface. In the presence of the SA medium, where the folding process is interrupted by segmentation with much smaller forces, the resulting surface shows no pit or crack defects [see Fig. 7(b)]. In fact, this drastic change in surface quality could also be ascertained by directly viewing the cut surface without any optical aids. Furthermore, the surface finish is improved by an order of magnitude—R_a for annealed Cu $\alpha = 0^\circ$ is 4.4 μm without media and 0.55 μm with glue 1.

E. Analytic model: mechanochemical effect as a local ductile-to-brittle transition

The observed mechanochemical effects of common SA media in metal cutting exhibit the three key characteristics that facilitate a ductile-to-brittle transition [34]—significant plastic deformation prior to fracture, crack nucleation during deformation, and a mechanism for surface energy reduction. Based on the observations, these are caused by fold initiation, notch formation at pinning points, and the applied SA medium, respectively. Each pinning point bounding a fold acts like a local stress concentrator or notch tip (see schematic in Fig. 8). In forming the chip, the tool imposes a remote shear τ_S on the workpiece. Within this framework, the transition from sinuous to segmentation-type flow corresponds to a competition between continued plastic deformation and unstable crack growth from O, respectively, in the presence of the SA medium. Quantitatively, this may be analyzed by considering the energetics of deformation at the tip O [35,36].

For the geometry and loading in Fig. 8, the elastic stress field at the tip of the notch is [37]

$$\sigma_{\rho\phi} = \frac{K_{\text{II}}}{2\sqrt{8\pi\rho}}\left[3\cos\frac{3\phi}{2} + \cos\frac{\phi}{2}\right], \quad K_{\text{II}} = \zeta\tau_S\sqrt{a}, \tag{1}$$

where ζ is a dimensionless constant that depends on the precise shape of the free surface on either side of the notch tip O. The applied shear τ_S increases continuously from the onset of plastic buckling and formation of the pinning point until it reaches a critical value τ_S^* for a crack of size a to grow from O, given by the Griffith criterion [38]

$$K_{\text{II}}^* = \zeta\tau_S^*\sqrt{a} = \sqrt{\frac{2E\gamma}{1-\nu^2}}, \tag{2}$$

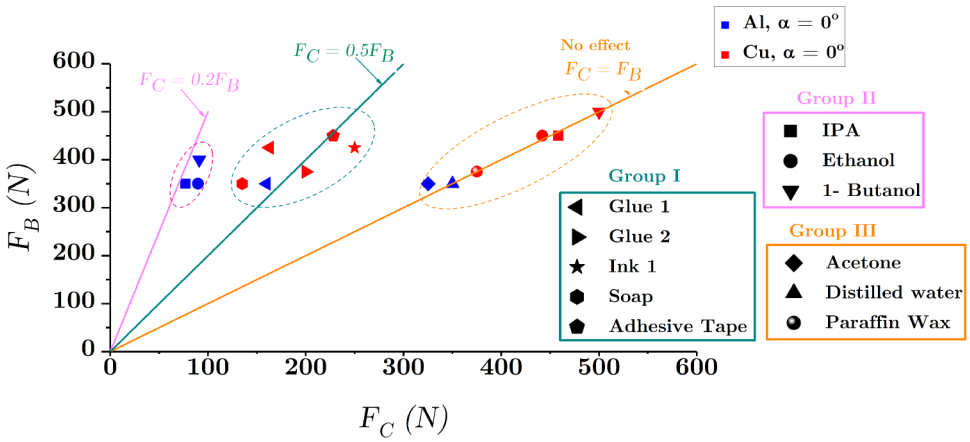

FIG. 4. Scatter plot showing cutting force values with (F_C) and without (F_B) media on various metals. The workpiece metals are indicated on the plot using different colors, whereas media are indicated using different symbols as specified in the legend. Group-I media fall around the $F_C = 0.5F_B$ line, group-II media on the $F_B = 0.2F_C$ line, and group-III media around the $F_B = F_C$ line (negligible mechanochemical effect). Al and Cu refer to metals in the annealed state.

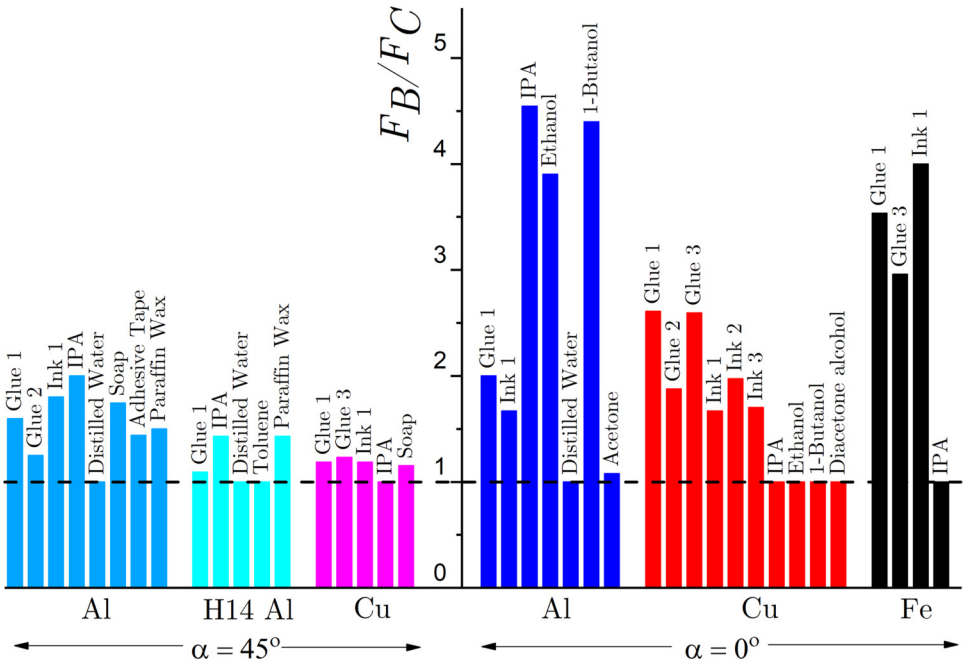

FIG. 5. Ratio of cutting force for uncoated (F_B) to SA-medium coated (F_C) workpiece samples for various SA media-metal combinations and cutting conditions. Mechanochemical effects result in force reductions of as much as 80% (Al-IPA, $\alpha = 0°$). Al, Cu, and Fe refer to metals in the annealed state, while H14 is a half-hard condition for Al.

where E and ν are the Young's modulus and Poisson's ratio, respectively, and γ is the surface energy. An adsorbed SA medium alters the surface properties, viz., γ in Eq. (2).

As opposed to crack growth at $\tau_S = \tau_S^*$, the metal may continue to deform plastically in the vicinity of O by continuous dislocation emission and crack blunting [35]. The net force acting on the dislocation shown in Fig. 8 may be divided into three primary contributions: the force F_τ due to the applied remote shear loading τ_S, an image force F_I due to traction-free boundary conditions on the crack surfaces, and a ledge force F_L due to the formation of the dislocation from the crack edge O [39].

The force F_τ may be evaluated using the expression $\vec{F}_{PK} = (\sigma \cdot \vec{b}) \times \hat{t}$, as follows:

$$\vec{F}_{PK} = \sigma_{\rho\phi} b_E = \left[\frac{E\gamma b}{4\pi(1-\nu^2)}\right]^{1/2} \frac{f(\phi)}{\sqrt{\xi}} \cos\psi\,\hat{\rho}. \quad (3)$$

Here, $\hat{t}$ and $\vec{b}$ represent the dislocation line direction and the Burgers vector, respectively, and ψ is the angle between them. The constants E, γ, and ν are the Young's modulus, surface energy, and Poisson's ratio, respectively. ξ is the dimensionless radius coordinate $\xi = \rho/b$. It is implicitly assumed in this expression that the remote shear stress τ_S is equal to the critical stress for crack growth. The function $f(\phi)$ is the material-independent expression for the angular dependence of the stress $\sigma_{\rho\phi}$:

$$f(\phi) = \frac{1}{2}\left[3\cos\frac{3\phi}{2} + \cos\frac{\phi}{2}\right]. \quad (4)$$

The image force on the dislocation may be computed directly, using thermodynamic arguments [39], as follows:

$$F_I = \vec{F}_i = -\frac{Eb(1-\nu\sin^2\psi)}{8\pi(1-\nu^2)}\frac{1}{\xi}\hat{\rho}. \quad (5)$$

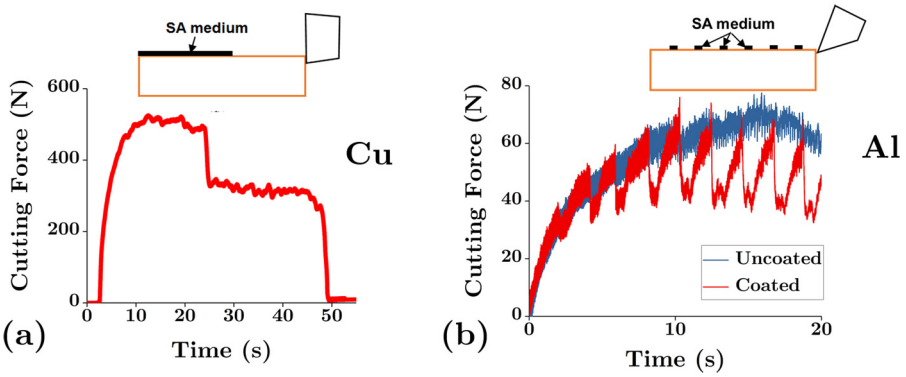

FIG. 6. Cutting forces reflect mechanochemical effects due to SA media. Forces for samples coated with SA media (a) along half the cutting length and (b) in a periodic spot pattern. The latter force oscillates at a frequency matching the spot spacing. Note that the cutting force is the force component in the direction of the velocity.

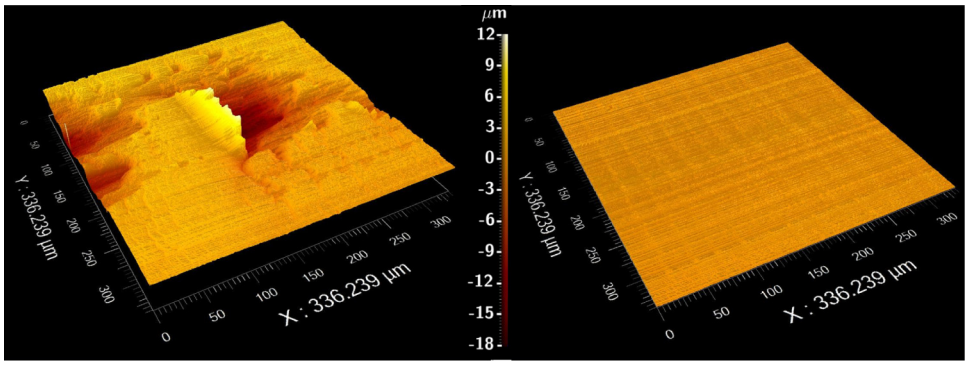

FIG. 7. Three-dimensional surface profiles showing the quality of the workpiece surface after cutting. (a) With sinuous flow, surface defects such as large pits (shown here) are very commonly observed. (b) With an SA medium, the transition to segmentation-type flow results in an order-of-magnitude improvement in surface quality and finish, as measured by the average pit size, pit density, and surface roughness (R_a).

Similarly, using the Peierls model of a dislocation with core radius ξ_C, the ledge force is approximated as follows [37]:

$$F_L = -\frac{2}{\pi}\frac{\gamma\alpha\cos\psi\sin\phi}{\xi^2+\alpha^2}, \quad \alpha = e^{3/2}\frac{\xi_C}{2}. \tag{6}$$

This force, F_L, is negligible when compared to F_I and F_τ, so that a good approximation for the equilibrium distance ξ^* is obtained by evaluating $F = F_I + F_\tau = 0$. The equilibrium distance ρ^* at which the two forces are balanced is then given by

$$\xi^* = \frac{\rho^*}{b} = \frac{(1-\nu\sin^2\psi)^2}{8\pi(1-\nu)}\frac{\mu b}{\gamma}\left(\frac{1}{f(\phi)\cos\psi}\right)^2, \qquad f(\phi) = \frac{1}{2}\left[3\cos\frac{3\phi}{2}+\cos\frac{\phi}{2}\right], \tag{7}$$

where $\mu = 2E/(1+\nu)$ is the shear modulus. This expression for ξ^* is determined purely by the notch geometry and material properties, and not by the loading τ_S. For a given configuration, the ability of the crack tip to emit dislocations along a certain direction ϕ, causing further plastic deformation without crack growth, is obtained by ξ^* and the dislocation core radius ξ_C: if $\xi^*/\xi_C > 1$, then any dislocation emitted at O must overcome an energy barrier to reach equilibrium at ξ^* and blunt the crack. In this case, crack growth from O is more favorable and segmentation-type flow ensues. On the other hand, if $\xi^*/\xi_C < 1$, then dislocation emission is favorable, so that the crack tip is blunted and the stress concentration lowered. Now $K_{\rm II} < K^*_{\rm II}$ and the crack does not grow from the pinning point O. Note that since pinning points coincide with ends of grain boundaries, and since dislocations are most easily emitted along these boundaries, ϕ approximately denotes the grain-boundary orientation.

The flow in the presence of an SA medium is easily predicted by comparing curves for $\xi^*(\phi)$ from Eq. (7) for different metal-media combinations. This is shown for bare or uncoated annealed Cu (black curve, surface energy $\gamma = \gamma_0$, $\mu b/\gamma_0 = 6.1$ [35]) in Fig. 9. An SA medium changes γ, depending on the strength of the metal-medium interface, resulting in a different $\xi^*(\phi)$ curve: see the plots for $\gamma = 0.5\gamma_0$, $0.2\gamma_0$, and $0.1\gamma_0$,

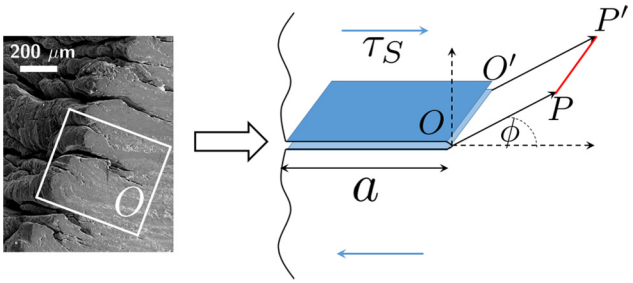

FIG. 8. Schematic of the model showing a fold pinning point (O) coinciding with the tip of a notch of length a, and causing increased local stress concentration under remote shear loading τ_S. Continued plastic deformation is enabled by emission of a dislocation (PP') from the tip OO' along a grain boundary oriented in the direction ϕ.

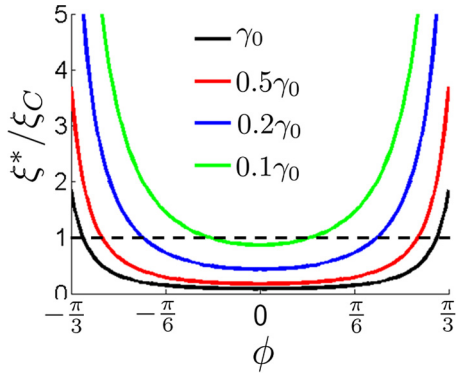

FIG. 9. Equilibrium dislocation distance ξ^*/ξ_C as a function of the grain-boundary orientation for varying surface energy γ. An order-of-magnitude change, from the uncoated metal (γ_0) to one with a suitable SA medium ($0.1\gamma_0$), favors crack growth as opposed to plastic deformation for nearly all grain-boundary orientations. This corresponds to a complete local transition from sinuous to segmentation-type flow, giving rise to the mechanochemical effect. Data are for Cu with $\mu b/\gamma_0 = 6.1$.

which are also shown in red, blue, and green, respectively. It is clear that for an order-of-magnitude change in γ, the $\xi^*(\phi)$ curve now almost entirely lies above the $\xi^*/\xi_C = 1$ line (dashed), so that crack growth along nearly all grain-boundary orientations is more favorable compared to continued plastic deformation. Thus, almost every pinning point should lead to segment formation (cf. Fig. 2, bottom row) in the presence of a strongly adhering SA medium. We have obtained a preliminary lower-bound estimate for $\gamma/\gamma_0 \approx 0.7$ from molecular-dynamics simulations for weakly adsorbed systems that demonstrated no mechanochemical effects (see the Appendix). Based on the experimental observations, it appears reasonable to expect $\gamma/\gamma_0 < 0.1$ for strongly adsorbing media such as glues and marking inks. Therefore, even with this conservative estimate of $\gamma = 0.2\gamma_0$ with SA media, the model predicts that it is favorable for crack growth to occur along directions $\phi > \pi/6$ (blue curve in Fig. 9).

IV. DISCUSSION

The observations show that a variety of chemical media, which adsorb strongly (physically) onto surfaces, cause significant reductions in the forces and energy when cutting soft metals, as highlighted by the results from cutting of Cu, Al, and Fe in an initially annealed condition (Figs. 4 and 5). This force and energy reduction can be taken as one key signature of the mechanochemical effect. It should be noted that while the term "mechanochemical" has been used for consistency with the literature [21], the interactions between the SA medium and the metal considered here mostly pertain to physisorption. The force and energy reductions are greatest with media that have the strongest adhesive interactions. For example, group-I media, which show strong adsorption with all three metals, cause force reductions typically of around 50% with all of the metals. This reduction is even greater with group-II media, which are known for strong adhesive interactions with Al alone; here, the force reduction is as high as 80% with Al. However, the group-II media have only a negligible influence on the force with annealed Cu and Fe, consistent with their known propensity to not adhere strongly to these metal surfaces. The results from group-III media further confirm this hypothesis, that with the absence of a strong adsorptive interaction with the metal surface, there is a negligible impact on the forces. It may be recalled that group-III media are characterized only by a weak interaction with all of the three metals. The force reductions observed with the group-I and -II media are also much greater than those reported in the past with CCl_4 as the chemical medium used in cutting [18–20]. The results thus show that strong adsorptive interaction of the medium with the metal surface is a necessary condition for the mechanochemical effect to be manifest in the cutting of metals.

Our experimental results also show that in addition to the strong adsorptive interaction between the media and the metal, a second condition is critical for the mechanochemical effect to occur. This condition is the need for sinuous flow, an unsteady flow mode, to prevail in the deformation zone. As seen from Fig. 2, this flow is characterized by large-amplitude material folding besides large strains. When the sinuous flow is much reduced or suppressed by changing the deformation geometry to $\alpha = 45^\circ$ (from $\alpha = 0^\circ$), or by prehardening the workpiece (H14 Al), the extent of the force reduction is significantly smaller or absent altogether (see Fig. 5). Under these conditions, smooth laminar (steady) flow becomes prevalent. The mechanochemical effect is now much smaller—indeed, in most cases, negligible—pointing to a strong coupling of the media action to the flow type.

The mechanism responsible for the major reduction in the forces with SA media is a transition in the deformation mode from sinuous flow, with material folding and excessive deformation, to a flow characterized by periodic fractures initiating from the metal surface—the segmentation-type flow. This transition in the flow—very much resembling a local ductile-to-brittle transition—is directly captured by the *in situ* imaging, and also predicted by a simple model of the deformation that incorporates key flow attributes (e.g., notch like features) and the energetics of the SA medium-metal interaction. The mere presence of the SA medium on the surface induces the metal to behave in a brittle manner during the deformation, when sinuous flow prevails, as with the annealed metals. The reason for this appears to be that sinuous flow produces stress-concentration features, locally, in the deformation zone that trigger local brittle behavior of the metal when the SA medium is present. As seen from the experimental observations, sinuous flow leads to the formation of mushroom-shaped features at the surface due to the folding [see Fig. 2(a)]. Interestingly, such folding has been reported to occur even at a nanometer length scale when cutting metals [40]. The pinning points between the folds are locations of high stress due to the notch like geometry (see Fig. 8). In addition, the SA medium acts to decrease the surface energy of the metal by adhering to it. The combination of the notched geometry and lowered surface energy allow for a crack to propagate from the notch tip, leading to a segmentation-type flow mode.

As shown in Sec. III.E, the presence of the SA medium at the tip of the notch embrittles the metal locally and allows for a crack to begin to propagate. Naturally, the question arises whether the SA medium is always in contact with the crack tip, as it propagates from the free surface toward the tool tip. While it has not been possible to track the penetration of the SA medium into the cracks during segment formation, the following scenario appears to be the most likely. The SA medium embrittles the material in the vicinity of the notch, making crack initiation at the

free surface favorable. Once a crack nucleates at the tip, it propagates naturally due to the dynamics of the loading, even through the tip itself might not subsequently contain the SA medium.

Per this crack-initiation mechanism, in the absence of crack-nucleation sites, such as pinning points on the surface, mechanochemical effects should not be observed. This is again consistent with the experimental observations. When laminar flow is the dominant deformation mode, then since the folding is absent, there are no notch like stress concentration features developing on the metal surface. Then, the surface energy reduction effected by the SA medium is likely not sufficient to cause the laminar flow to transition to a segmentation-type flow. Under these conditions, a noticeable force reduction is not observed with the SA media: see the results for hardened Al (H14) and $\alpha = 0^\circ$ for annealed Cu and Al (Fig. 5). In fact, similar behavior with regard to the presence of defect features on the initial surface has also been observed in the case of liquid-metal embrittlement [16]. It is thus suggested that the action of the SA medium is to effect a local ductile-to-brittle transition. The beneficial consequences of ensuing flow transition are significant—smaller forces, energies and strains in surface generation, and an order-of-magnitude improvement in surface quality as measured by surface topography and defect density.

We have seen the mechanochemical effect to prevail when sinuous flow occurs, because this type of unsteady flow provides the impetus for fracture instabilities to occur via crack nucleation at suitable surface pinning points. This raises a broader scientific question as to whether similar flow or fracture transitions, with beneficial effects, can be effected with other unsteady deformation modes such as shear banding. Such modes are not infrequently observed in deformation processing and include analogous pinning points. This question is currently under study.

The mechanochemical effect described in this study is somewhat unique in that it is not material specific. Since the effect is observed not only with glues of different chemical compositions (cf. glues 1, 2, and 3), but also with other media such as inks, it points to the fact that the bonds that form between the medium and the metal cannot be material specific but arise due to electrostatic interactions. It is well known that bonds that form between glues and metal surfaces, mediated by the van der Waals force, are precisely of this nature [30].

Given that glues and inks adhere to nearly all metals, the beneficial effects of surface-active media demonstrated herein should open up new opportunities in cutting, stamping, piercing, and forming of soft and highly-strain-hardening metals such as Fe, Al, Ta, stainless steels, and Ni alloys. These metals are well known as being just as difficult to process as hard metals, though, because of their softness. The benign nature of the surface-active media—in fact, most of these are commonly used in everyday life and household practice—also means that this effect can be easily implemented in industrial settings.

V. CONCLUSIONS

A mechanochemical effect in cutting and large-strain deformation of metals is demonstrated using high-speed *in situ* imaging of deformation and flow, complemented by force measurements. In cutting of soft metals and highly-strain-hardening metals such as aluminum, copper, and iron, this effect is characterized by reduction in cutting forces and energy by up to 80% when a suitable chemical surface-active medium is merely coated onto the metal surface prior to the cutting. The key conditions for the effect to be manifest are (a) strong physical adsorption (adhesion) of the medium to the metal surface and (b) the occurrence of an unsteady plastic-flow mode—sinuous flow—characterized by large-amplitude folding and large strains. This mechanochemical effect is distinguished from other catastrophic mechanochemical effects such as liquid-metal embrittlement and stress-corrosion cracking in that it is controllable, not material specific, and effected by common household media such as glues and inks. Another unique feature is coupling of the media action to the flow mode. The mechanism underlying the effect and force reduction is a transition in the deformation mode—from sinuous flow, which commonly prevails in the cutting of these highly-strain-hardening metals, to a segmentation-type flow in the presence of the chemical medium. Direct observations and modeling show this flow transition to occur via a local change in the behavior of the metal surface from ductile to brittle, which arises from a lowering of the surface energy of the metal and the formation of notch like features due to the folding from the sinuous flow. Concomitant with the flow transition and force reduction, an order-of-magnitude improvement in the quality of the cut surface has been observed. The benign nature and simplicity of the media with which these beneficial effects are observed suggests interesting possibilities for enhancing the performance of cutting and forming processes for metal alloys.

ACKNOWLEDGMENTS

The authors would like to acknowledge support from US Army Research Office Award No. W911NF-15-1-0591, NSF Grants No. PCMMI 1562470 and No. DMR 1610094, and the US Department of Energy EERE program via Award No. DE-EE0007868.

APPENDIX: ATOMISTIC SIMULATIONS FOR SURFACE ENERGY ESTIMATES

Metal-media interactions are studied using molecular-dynamics simulations, performed using the open-source

software LAMMPS [41]. The specific aim of these simulations is to estimate the change in surface energy of the metal due to contact with a typical SA agent. Change in surface energy is related to the strength of bonds that develop between the metal and the media. In order to predict the formation of any potential bonds, the ReaxFF potential is used [42]. Due to the limited availability of data on potentials for SA media and metals, the surface energy calculations are done for the interaction between isopropyl alcohol and pure Fe alone, for which potentials are available.

An orthorhombic box ($7 \times 7 \times 3$ nm^3) containing Fe atoms in a bcc lattice is created with a lattice parameter of 2.856 Å. Periodic boundary conditions are imposed in the X and Y directions, while the box is bounded in the Z direction by free surfaces whose properties are to be studied. A time step of 0.25 fs is used and the system temperature is maintained at 300 K using a Langevin thermostat. The system of Fe atoms is equilibrated (as indicated by the total energy) by running the simulation for 20 000 time steps. In a separate simulation, isopropyl alcohol molecules are generated using the Avagadro software. They are then equilibrated by running the simulation in LAMMPS for 20 000 time steps and monitoring the energy of the system.

The surface energy is calculated using the virial stress method [43,44].This approach calculates the change in the stress in a direction perpendicular to the interface, due to the surface tension forces. The surface (interface) energy is calculated using the following formula:

$$\gamma = \frac{L_z}{2}\left[P_{zz} - \left(\frac{P_{xx} + P_{yy}}{2}\right)\right], \tag{A1}$$

Here, γ refers to the surface or interface energy, L_z to the length of the orthorhombic box in the Z direction, and P_{ii} to the ith component of the stress tensor.

The surface energy of pure Fe, computed using this procedure, is obtained as 2.19 J/m^2, which is close to the value that is usually reported [45]. The estimate is verified to be independent of system size by obtaining similar results for a box of different dimensions ($4.8 \times 4.8 \times 1.5$ nm^3).

Next, IPA molecules are introduced into the orthorhombic cell containing the Fe atoms, so that they could interact with the surfaces normal to the Z direction. The Fe-IPA system is allowed to equilibrate (as determined by total system energy) by running the simulation for 20 000 time steps. Using Eq. (1) again, the value of the interface energy between Fe and IPA is calculated to be 1.64 J/m^2. This represents a decrease in the surface energy by 28%. It is expected that with molecules that adsorb strongly to the Fe surface, such as glues, the drop will be much greater.

[1] J. E. Williams, E. F. Smart, and D. R. Milner, Metallurgy of machining. Part 1: Basic considerations and the cutting of pure metals, Metallurgia **81**, 3 (1970).

[2] H. Yeung, K. Viswanathan, W. D. Compton, and S. Chandrasekar, Sinuous flow in metals, P. Natl Acad. Sci. USA **112**, 9828 (2015).

[3] G. Schneider, *Machinability of Metals* (American Machinist, 2009).

[4] K. Viswanathan, A. Udupa, H. Yeung, D. Sagapuram, J. B. Mann, M. Saei, and S. Chandrasekar, On the stability of plastic flow in cutting of metals, CIRP Ann. Manuf. Technol. **66**, 69 (2017).

[5] A. Udupa, K. Viswanathan, Y. Ho, and S. Chandrasekar, The cutting of metals via plastic buckling, Proc. R. Soc. A **473**, 20160863 (2017).

[6] H. Yeung, K. Viswanathan, A. Udupa, A. Mahato, and S. Chandrasekar, Sinuous Flow in Cutting of Metals, Phys. Rev. Appl. **8**, 054044 (2017).

[7] Pliny, *Natural History* (1847) translated by Philemon Holland.

[8] K. H. Brown, D. A. Grose, R. C. Lange, T. H. Ning, and P. A. Totta, Advancing the state of the art in high-performance logic and array technology, IBM J. Res. Dev. **36**, 821 (1992).

[9] M. Krishnan, J. W. Nalaskowski, and L. M. Cook, Chemical mechanical planarization: Slurry chemistry, materials, and mechanisms, Chem. Rev. **110**, 178 (2009).

[10] A. R. C. Westwood, N. M. Macmillan, and R. S. Kalyoncu, Chemomechanical phenomena in hard rock drilling, Int. J. Rock Mech. Min. Sci. **11** (11), A233 (1974).

[11] A. R. C. Westwood and J. J. Mills, in *Surface Effects in Crystal Plasticity*, edited by R. M. Latanision and J. T. Fourie (Nordhoff, Leyden, 1977) see also discussion by A. Argon, following the article

[12] O. Reynolds, Chem. News 29, 117 (1874); mem, Proceedings of the Literary and Philosophical Society of Manchester 13, 93 (1874)

[13] W. D. Robertson, *Stress, Corrosion Cracking and Embrittlement* (J. Wiley, New York, 1956).

[14] W. Rostoker, J. McCaughey, and H. Markus, *Embrittlement by Liquid Metals* (Reinhold Pub. Corp., New York, 1960).

[15] A. Westwood and M. Kamdar, Concerning liquid metal embrittlement, particularly of zinc monocrystals by mercury, Philos. Mag. **8**, 787 (1963).

[16] P. Fernandes and D. Jones, Specificity in liquid metal induced embrittlement, Eng. Fail. Anal. **3**, 299 (1996).

[17] P. Rehbinder, New physico-chemical phenomena in the deformation and mechanical treatment of solids, Nature **159**, 866 (1947).

[18] E. Usui, A. Gujral, and M. C. Shaw, An experimental study of the action of CCl_4 in cutting and other processes involving plastic flow, Int. J. Mach. Tool Design Res. **1**, 187 (1961).

[19] E. M. Kohn, Role of extreme pressure lubricants in boundary lubrication and in metal cutting, Nature **197**, 895 (1963).

[20] P. L. Barlow, Rehbinder effect in lubricated metal cutting, Nature **211**, 1076 (1966).

[21] P. A. Rehbinder and E. D. Shchukin, Surface phenomena in solids during deformation and fracture processes, Prog. Surf. Sci. **3**, 97 (1972).
[22] E. D. Shchukin, The influence of surface-active media on the mechanical properties of materials, Adv. Colloid Interface Sci. **123**, 33 (2006).
[23] J. R. Rice, in *Chemistry and Physics of Fracture*, edited by R. M. Latanision and R. H. Jones (Martinus Nijhoff, Boston, 1987) pp. 23.
[24] R. M. Latanision, in *Surface Effects in Crystal Plasticity*, edited by R. M. Latanision and J. T. Fourie (Nordhoff, Leyden, 1977).
[25] C. Cassin and G. Boothroyd, Lubricating action of cutting fluids, J. Mech. Eng. Sci. **7**, 67 (1965).
[26] K. Nakayama, in *Proceedings of International Conference on Production Engineering* (1974) pp. 572.
[27] By the same token, some surfactants may also be termed surface-active. We use the term surface-active (SA) throughout the paper.
[28] K. Viswanathan, A. Mahato, H. Yeung, and S. Chandrasekar, Surface phenomena revealed by *in situ* imaging: Studies from adhesion, wear and cutting, Surf. Topogr. Metrol. Prop. **5**, 014002 (2017).
[29] G. Gottstein, A. King, and L. Shvindlerman, The effect of triple-junction drag on grain growth, Acta Mater. **48**, 397 (2000).
[30] E. M. Petrie, *Handbook of Adhesives and Sealants* (McGraw–Hill, New York, 2007).
[31] A. R. Anderson and W. E. Smith, Processes for preparing metal alkyls and alkoxides, US Patent 2,965,663 (1960).
[32] O. Helmboldt, L. Keith Hudson, C. Misra, K. Wefers, W. Heck, H. Stark, M. Danner, and N. Rösch. Aluminum compounds, inorganic, in *Ullmann's Encyclopedia of Industrial Chemistry* (Wiley-VCH Verlag GmbH & Co. KGaA, 2000).
[33] A. Mahato, Y. Guo, N. K. Sundaram, and S. Chandrasekar, Surface folding in metals: A mechanism for delamination wear in sliding, Proc. R. Soc. A **470**, 20140297 (2014).
[34] A. H. Cottrell, Theory of brittle fracture in steel and similar metals, T. Metall. Soc. AIME **212**, 192 (1958).
[35] J. R. Rice and R. Thomson, Ductile versus brittle behaviour of crystals, Philos. Mag. **29**, 73 (1974).
[36] B. Bilby, A. Cottrell, and K. Swinden, The spread of plastic yield from a notch, Proc. R. Soc. A **272**, 304 (1963).
[37] M. Williams, The bending stress distribution at the base of a stationary crack, J. Appl. Mech. **24**, 109 (1957).
[38] J. F. Knott, *Fundamentals of Fracture Mechanics* (Butterworths, London, 1973).
[39] J. Hirth and J. Lothe, *Theory of Dislocations* (McGraw-Hill, New York, 1968).
[40] N. Beckmann, P. Romero, D. Linsler, M. Dienwiebel, U. Stolz, M. Moseler, and P. Gumbsch, Origins of Folding Instabilities on Polycrystalline Metal Surfaces, Phys. Rev. Appl. **2**, 064004 (2014).
[41] S. Plimpton, Fast parallel algorithms for short-range molecular dynamics, J. Comput. Phys. **117**, 1 (1995).
[42] M. Aryanpour, A. C. van Duin, and J. D. Kubicki, Development of a reactive force field for iron-oxyhydroxide systems, J. Phys. Chem. A **114**, 6298 (2010).
[43] U. O. M. Vázquez, W. Shinoda, P. B. Moore, C.-C. Chiu, and S. O. Nielsen, Calculating the surface tension between a flat solid and a liquid: A theoretical and computer simulation study of three topologically different methods, J. Math. Chem. **45**, 161 (2009).
[44] T. L. Hill, *An Introduction to Statistical Thermodynamics* (Addison-Wesley, Reading, 1960).
[45] S. Schönecker, X. Li, B. Johansson, S. K. Kwon, and L. Vitos, Thermal surface free energy and stress of Iron, Sci. Rep. **5**, 14860 (2015).